

Predictions of hadronic observables in $Pb + Pb$ collisions at $\sqrt{s_{NN}} = 2.76$ TeV from a hadronic rescattering model

T. J. Humanic*

Department of Physics, The Ohio State University, Columbus, Ohio, USA

(Dated: November 12, 2018)

Abstract

A kinematic model based on the superposition of $p + p$ collisions, relativistic geometry and final-state hadronic rescattering is used to predict various hadronic observables in $\sqrt{s_{NN}} = 2.76$ TeV $Pb + Pb$ collisions. Predictions for rapidity and transverse momentum distributions, elliptic flow, and two-boson femtoscopy are presented. A short proper time for hadronization is assumed. Previous calculations using this model which were performed for $\sqrt{s_{NN}} = 200$ GeV $Au + Au$ collisions were shown to describe reasonably well the trends of observables in experiments carried out at that energy, giving the present predictions for $Pb + Pb$ at higher energy some degree of credibility.

PACS numbers: 25.75.Dw, 25.75.Gz, 25.40.Ep

arXiv:1011.0378v1 [nucl-th] 1 Nov 2010

* humanic@mps.ohio-state.edu

I. INTRODUCTION

The present plan for running at the CERN Large Hadron Collider (LHC) calls for $Pb+Pb$ collisions at $\sqrt{s_{NN}} = 2.76$ TeV to commence in November, 2010. These will be the highest energy heavy ion collisions ever produced in the laboratory, and it is hoped that exotic phenomena will be observed which will expand our knowledge of the properties of highly excited matter [1].

In this context, it is the goal of the present paper to make predictions for common hadronic observables which will be initially measured by LHC experiments in these high-energy $Pb+Pb$ collisions. Predictions for spectra (i.e. rapidity and transverse momentum distributions), elliptic flow, and two-boson femtoscopy are presented. A hadronic rescattering model in which the initial state is determined by the superposition of proton-proton collisions has been chosen to make these predictions. The advantages of this model for this purpose are 1) the model has been shown to describe the overall trends of hadronic observables in lower energy $Au+Au$ collisions at $\sqrt{s_{NN}} = 0.20$ TeV from the Relativistic Heavy Ion Collider (RHIC)[2], and 2) the model is easily scalable to LHC energies. These will be “limiting case scenario” predictions in the sense that only hadrons are used as the degrees of freedom in this model even at the early stages of the collision where parton degrees of freedom are thought to be more appropriate, i.e. a short proper time for hadronization is assumed.

The paper is organized into the following sections: Section II gives a brief description of the model, Section III presents predictions from the model for $\sqrt{s_{NN}} = 2.76$ TeV $Pb+Pb$ collisions, and Section IV gives a summary and conclusions.

II. DESCRIPTION OF THE MODEL

The model calculations are carried out in five main steps: A) generate hadrons in $p+p$ collisions from PYTHIA, B) superpose $p+p$ collisions in the geometry of the colliding nuclei, C) employ a simple space-time geometry picture for the hadronization of the PYTHIA-generated hadrons, D) calculate the effects of final-state rescattering among the hadrons, and E) calculate the hadronic observables. These steps will now be discussed in more detail.

A. Generation of the $p + p$ collisions with PYTHIA

The $p + p$ collisions were modeled with the PYTHIA code [3], version 6.409. The internal parton distribution functions “CTEQ 5L” (leading order) were used in these calculations. Events were generated in “minimum bias” mode, i.e. setting the low- p_T cutoff for parton-parton collisions to zero (or in terms of the actual PYTHIA parameter, $ckin(3) = 0$) and excluding elastic and diffractive collisions (PYTHIA parameter $m_{sel} = 1$). Runs were made at $\sqrt{s} = 2.76$ TeV to simulate the upcoming LHC collisions. Information saved from a PYTHIA run for use in the next step of the procedure were the momenta and identities of the “direct” (i.e. redundancies removed) hadrons (all charge states) π , K , p , n , Δ , Λ , ρ , ω , η , η' , ϕ , and K^* . These particles were chosen since they are the most common hadrons produced and thus should have the greatest effect on the hadronic observables in these calculations.

B. Superposition of $p + p$ events to simulate heavy-ion collisions

An assumption of the model is that an adequate job of describing the heavy-ion collision can be obtained by superposing PYTHIA-generated $p + p$ collisions calculated at the beam \sqrt{s} within the collision geometry of the colliding nuclei. Specifically, for a collision of impact parameter b , if $f(b)$ is the fraction of the overlap volume of the participating parts of the nuclei such that $f(b = 0) = 1$ and $f(b = 2R) = 0$, where $R = 1.2A^{1/3}$ and A is the mass number of the nuclei, then the number of $p + p$ collisions to be superposed will be $f(b)A$. The positions of the superposed $p + p$ pairs are randomly distributed in the overlap volume and then projected onto the $x - y$ plane which is transverse to the beam axis defined in the z -direction. The coordinates for a particular $p + p$ pair are defined as x_{pp} , y_{pp} , and $z_{pp} = 0$. The positions of the hadrons produced in one of these $p + p$ collisions are defined with respect to the position so obtained of the superposed $p + p$ collision (see below).

As was done in similar calculations for RHIC collisions to give better agreement with experimental $dn/d\eta$ distributions[2], a lower multiplicity cut was applied to the $p + p$ collisions used in the present calculations which rejected the lowest 20% of the events. The spirit of this cut is to partially compensate for the fact that there is no reinteraction of primary nucleons from the projectile-target system in this model.

C. The space-time geometry picture for hadronization

The space-time geometry picture for hadronization from a superposed $p + p$ collision located at (x_{pp}, y_{pp}) consists of the emission of a PYTHIA particle from a thin uniform disk of radius 1 fm in the $x - y$ plane followed by its hadronization which occurs in the proper time of the particle, τ . The space-time coordinates at hadronization in the lab frame (x_h, y_h, z_h, t_h) for a particle with momentum coordinates (p_x, p_y, p_z) , energy E , rest mass m_0 , and transverse disk coordinates (x_0, y_0) , which are chosen randomly on the disk, can then be written as

$$x_h = x_{pp} + x_0 + \tau \frac{p_x}{m_0} \quad (1)$$

$$y_h = y_{pp} + y_0 + \tau \frac{p_y}{m_0} \quad (2)$$

$$z_h = \tau \frac{p_z}{m_0} \quad (3)$$

$$t_h = \tau \frac{E}{m_0} \quad (4)$$

Eqs. (1) and (2) show the initial expansion in the transverse direction now present in the model. The simplicity of this geometric picture is now clear: it is just an expression of causality with the assumption that all particles hadronize with the same proper time, τ . A similar hadronization picture (with an initial point source) has been applied to $e^+ - e^-$ collisions[4]. For all results presented in this work, τ will be set to 0.1 fm/c as was done in applying the present model to calculating predictions for RHIC $Au + Au$ collisions[2] and Tevatron $p + \bar{p}$ collisions[5].

D. Final-state hadronic rescattering

The hadronic rescattering calculational method used is similar to that employed in previous studies [6, 7]. Rescattering is simulated with a semi-classical Monte Carlo calculation which assumes strong binary collisions between hadrons. Relativistic kinematics is used throughout. The hadrons considered in the calculation are the most common ones: pions, kaons, nucleons and lambdas (π , K, N, and Λ), and the ρ , ω , η , η' , ϕ , Δ , and K^* resonances. For simplicity, the calculation is isospin averaged (e.g. no distinction is made among a π^+ , π^0 , and π^-).

The rescattering calculation finishes with the freeze out and decay of all particles. Starting from the initial stage ($t = 0$ fm/c), the positions of all particles in each event are allowed to evolve in time in small time steps ($\Delta t = 0.5$ fm/c) according to their initial momenta. At each time step each particle is checked to see a) if it has hadronized ($t > t_h$, where t_h is given in Eq. (4)), b) if it decays, and c) if it is sufficiently close to another particle to scatter with it. Isospin-averaged s-wave and p-wave cross sections for meson scattering are obtained from Prakash et al.[8] and other cross sections are estimated from fits to hadron scattering data in the Review of Particle Physics[9]. Both elastic and inelastic collisions are included. The calculation is carried out to 400 fm/c which allows enough time for the rescattering to finish (as a test, calculations were also carried out for longer times with no changes in the results). Note that when this cutoff time is reached, all un-decayed resonances are allowed to decay with their natural lifetimes and their projected decay positions and times are recorded.

The rescattering calculation is described in more detail elsewhere [6, 7]. The validity of the numerical methods used in the rescattering code have been studied using the subdivision method, the results of which have verified that the methods used are valid [10].

E. Calculation of the hadronic observables

Model runs are made to be “minimum bias” by having the impact parameters of collisions follow the distribution $d\sigma/db \propto b$, where $0 < b < 2R$. Observables are then calculated from the model in the appropriate centrality bin by making multiplicity cuts as normally done in experiments, as well as kinematic cuts on rapidity and p_T . For the present study, a full-calculation 3200 event minimum bias run was made from the model for $\sqrt{s_{NN}} = 2.76$ TeV $Pb + Pb$ collisions which was then used to calculate all of the hadronic observables shown. In addition, a 3200 event minimum bias run with rescattering turned off in the model was also made for comparison to study the importance of rescattering in these observables.

III. PREDICTIONS FOR $\sqrt{s_{NN}} = 2.76$ TEV $Pb + Pb$ COLLISIONS

As mentioned earlier, predictions for the hadronic observables spectra, elliptic flow, and two-boson femtoscopy have been made with the present model for $\sqrt{s_{NN}} = 2.76$ TeV $Pb+Pb$ collisions. Results for each of these observables are presented separately below.

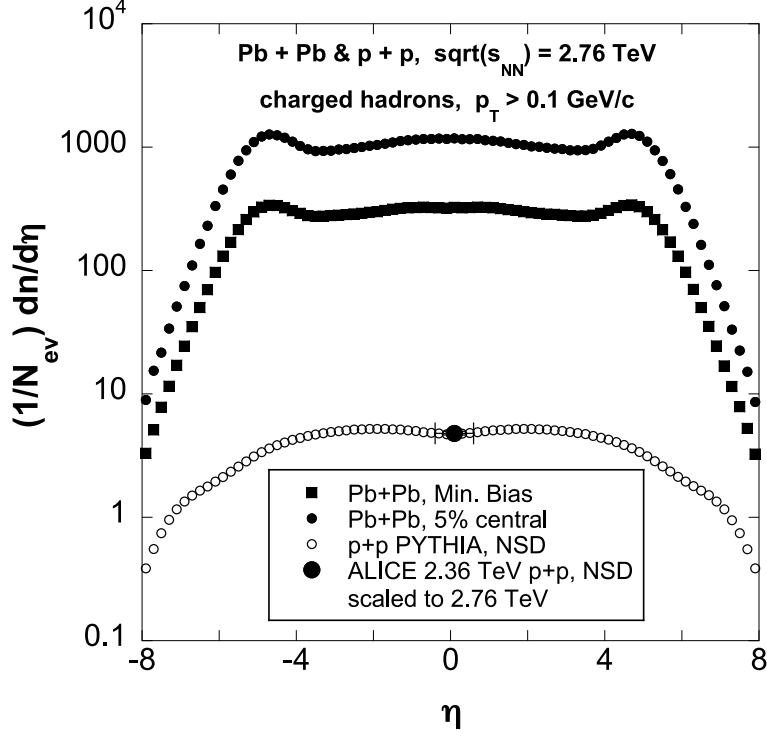


FIG. 1. Model charged-hadron pseudorapidity distributions for $Pb + Pb$ collisions at $\sqrt{s_{NN}} = 2.76$ TeV for minimum bias and 0 – 5% centrality bins. Also shown is a comparison of non-single diffractive PYTHIA $p + p$ collisions at $\sqrt{s} = 2.76$ TeV with a measurement from ALICE scaled to this energy.

A. Spectra

Figures 1, 2, and 3 show predictions from the present model for charged hadron spectra. Figure 1 shows charged-hadron pseudorapidity distributions for $Pb + Pb$ collisions at $\sqrt{s_{NN}} = 2.76$ TeV for minimum bias and 0 – 5% centrality bins. Also shown is a comparison of non-single diffractive PYTHIA $p + p$ collisions at $\sqrt{s} = 2.76$ TeV with a measurement of non-single-diffractive $dn/d\eta$ from the LHC ALICE experiment made at $\sqrt{s} = 2.36$ TeV [11], approximately scaled to the slightly higher energy by $\sqrt{2.76/2.36}$. Since the model is “isospin averaged”, the model distributions are multiplied by $2/3$ to approximate all charged particles. Looking at the $p + p$ distribution first, it is seen that PYTHIA is in good agreement with the scaled ALICE measurement at mid-rapidity, giving additional confidence in using PYTHIA $p + p$ collisions at this energy in the superposition for the $Pb + Pb$ collisions. Looking at the distributions for $Pb + Pb$, the mid-rapidity $dn/d\eta$ values for minimum bias

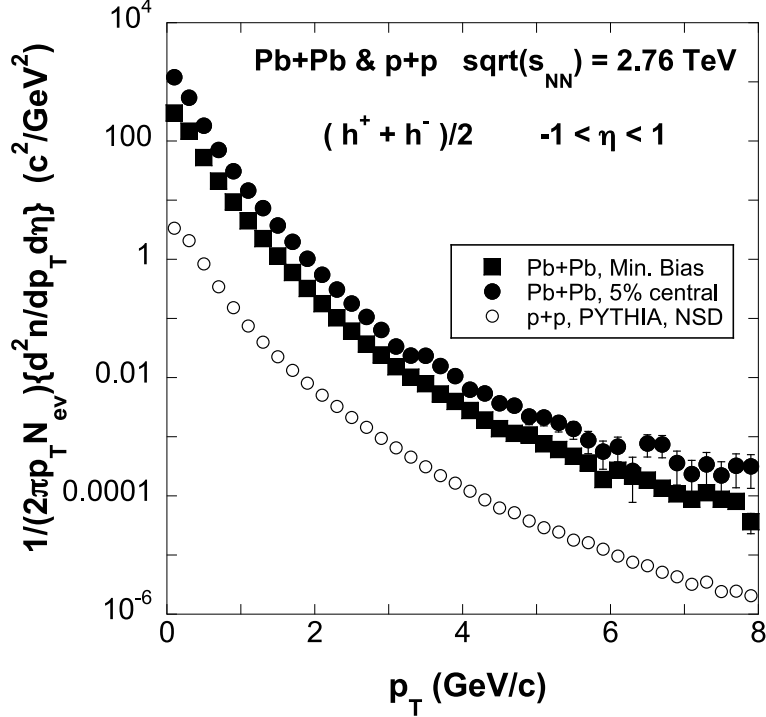


FIG. 2. Model charged-hadron p_T distributions for the same conditions as shown in Figure 1.

and central collisions are found to be 323 and 1174, respectively. For central collisions, this is about twice the value found in RHIC $\sqrt{s_{NN}} = 200$ GeV $Au + Au$ collisions [12], and it is at the lower end of the range of predictions which have been recently made of 1500 – 4000 in central collisions using various extrapolations of RHIC experimental rapidity densities [1].

Figure 2 shows charged-hadron p_T distributions for $Pb+Pb$ collisions at $\sqrt{s_{NN}} = 2.76$ TeV for minimum bias and 0–5% centrality bins. Also shown for comparison is the p_T distribution for non-single diffractive PYTHIA $p + p$ collisions at $\sqrt{s} = 2.76$ TeV. To approximate $(h^+ + h^-)/2$ for the model, the model distributions are multiplied by 1/3. The 0 – 5% centrality charged particle p_T distribution for $p_T > 5$ GeV/c is predicted to be about two orders of magnitude larger at the LHC compared with RHIC [13]. This is an expected consequence of the higher $\sqrt{s_{NN}}$ in the LHC collisions that the p_T distributions at high p_T should be greatly enhanced.

Figure 3 shows the ratio of minimum bias $Pb + Pb$ to $p + p$ p_T distributions from Figure 2 (indicated as “Rescattering ON”). Also shown for comparison is the similar ratio with rescattering turned off in the model. This ratio is essentially the “unnormalized” R_{AA} observable[14]. Studying the high p_T behavior of R_{AA} is thought to be a way of more directly

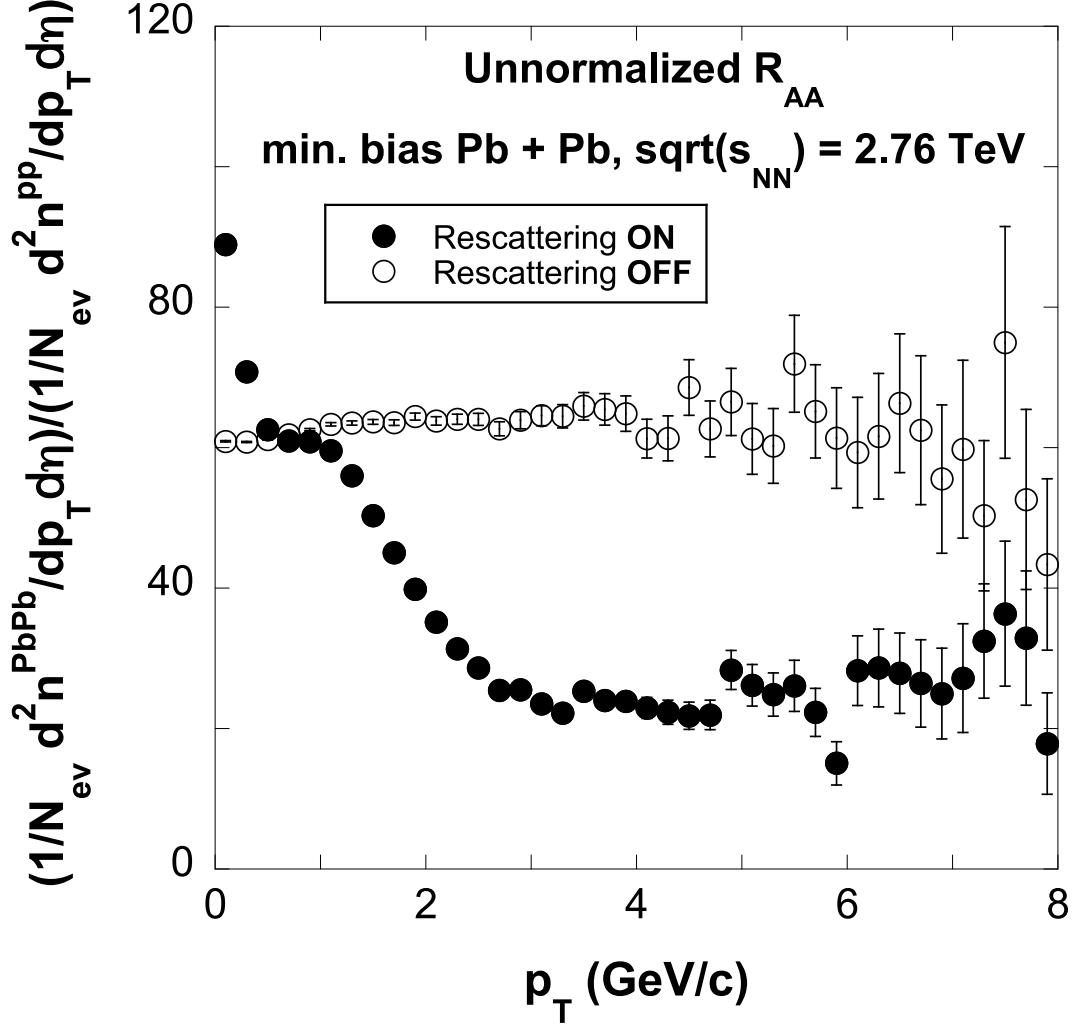


FIG. 3. Ratio of minimum bias $Pb + Pb$ to $p + p$ p_T distributions from Figure 2 (indicated as “Rescattering ON”). Also shown is the similar ratio with rescattering turned off in the model.

studying QCD processes, such as jets, in heavy-ion collisions. Since the present model is based on using PYTHIA which uses QCD processes in calculating $p + p$ collisions, the model should contain these effects and thus should be suitable for comparing with experiments which measure these observables. As seen in Figure 3, for the full rescattering calculation the ratio is suppressed for $p_T > 2$ GeV/c compared with the case of rescattering turned off. This high- p_T suppression is similar to that observed in RHIC collisions[14]. In the present model calculations this suppression is clearly seen to be due to hadronic rescattering.

B. Elliptic flow

The elliptic flow variable, V_2 , is defined as

$$V_2 = \langle \cos(2\phi) \rangle \tag{5}$$

$$\phi = \arctan\left(\frac{p_y}{p_x}\right)$$

where “ $\langle \rangle$ ” implies a sum over particles in an event and a sum over events and where p_x and p_y are the x and y components of the particle momentum, and x is in the impact parameter direction, i.e. reaction plane direction, and y is in the direction perpendicular to the reaction plane. The V_2 variable is calculated from the model using Eq. (5) and taking the reaction plane to be the model $x - z$ plane.

Figure 4 shows model V_2 vs. p_T plots for $\sqrt{s_{NN}} = 2.76$ TeV $Pb + Pb$ collisions for minimum bias and 0 – 5% centrality bins, all hadrons, and $-1 < \eta < 1$. Also shown is the minimum bias case with rescattering turned off. For the minimum bias case with the full calculation, V_2 is seen to increase with increasing p_T , peaking at a value of about 0.14 and then decreasing for p_T increasing beyond 2.5 GeV/c. For the 0 – 5% centrality case, V_2 is also seen to increase with increasing p_T and to have a significantly smaller magnitude than the minimum bias case. These general behaviors of V_2 are also observed in RHIC collisions[15, 16]. When rescattering is turned off, $V_2 \rightarrow 0$ for all p_T , demonstrating that hadronic rescattering accounts completely for the elliptic flow signal in this model.

C. Two-boson femtoscopy (Hanbury-Brown-Twiss interferometry)

Figures 5-9 and Tables I-III show predictions from the model for two-pion and two-kaon HBT for $\sqrt{s_{NN}} = 2.76$ TeV $Pb + Pb$ collisions. For the HBT[17] calculations from the model, the three-dimensional two-boson correlation function is formed and a Gaussian function in momentum difference variables is fitted to it to extract the boson source parameters. Boson statistics are introduced after the rescattering has finished (i.e. when all particles have “frozen out”) using the standard method of pair-wise symmetrization of bosons in a plane-wave approximation [18]. The three-dimensional correlation function, $C(Q_{side}, Q_{out}, Q_{long})$, is then calculated in terms of the momentum-difference variables Q_{side} , which points in the direction of the sum of the two boson momenta in the transverse plane, Q_{out} , which points

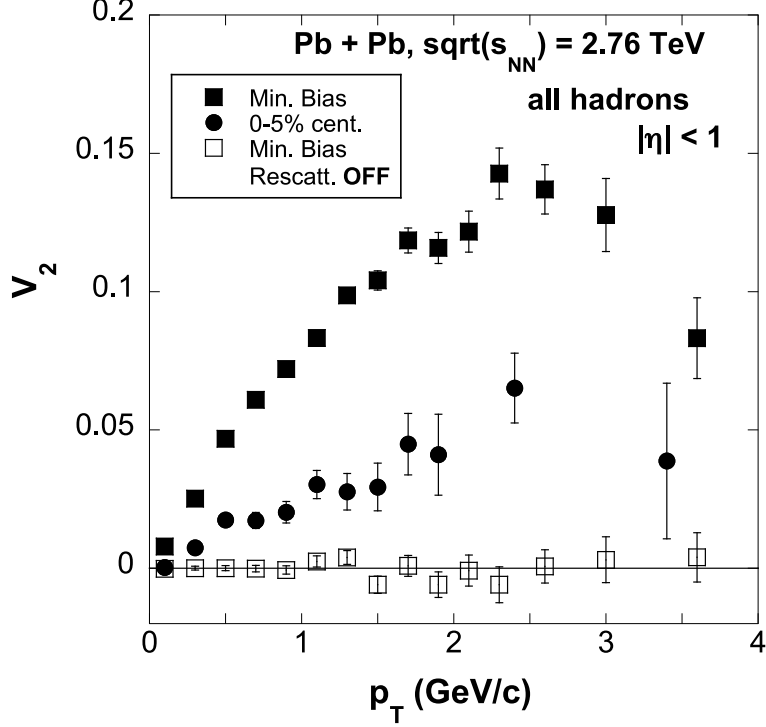


FIG. 4. Model V_2 vs. p_T plots for $Pb + Pb$ collisions for minimum bias and 0 – 5% centrality bins, all hadrons, and $-1 < \eta < 1$. Also shown is the minimum bias case with rescattering turned off.

perpendicular to Q_{side} in the transverse plane and the longitudinal variable along the beam direction Q_{long} .

The final step in the calculation is extracting fit parameters by fitting a Gaussian parameterization to the model-generated two-boson correlation function given by, [19]

$$C(Q_{side}, Q_{out}, Q_{long}) = G[1 + \lambda \exp(-Q_{side}^2 R_{side}^2 - Q_{out}^2 R_{out}^2 - Q_{long}^2 R_{long}^2)] \quad (6)$$

where the R -parameters, called the radius parameters, are associated with each momentum-difference variable direction, G is a normalization constant, and λ is the usual empirical parameter added to help in the fitting of Eq. (6) to the actual correlation function ($\lambda = 1$ in the ideal case). The fit is carried out in the conventional LCMS frame (longitudinally comoving system) in which the longitudinal boson pair momentum vanishes [19]. Figure 5 shows a sample projected two-pion correlation function from the model with projected fit to Eq. (6). It is seen that Eq. (6) fits the model-generated correlation function quite well.

Figure 6 shows the dependence of the model pion source parameters for $Pb + Pb$ collisions

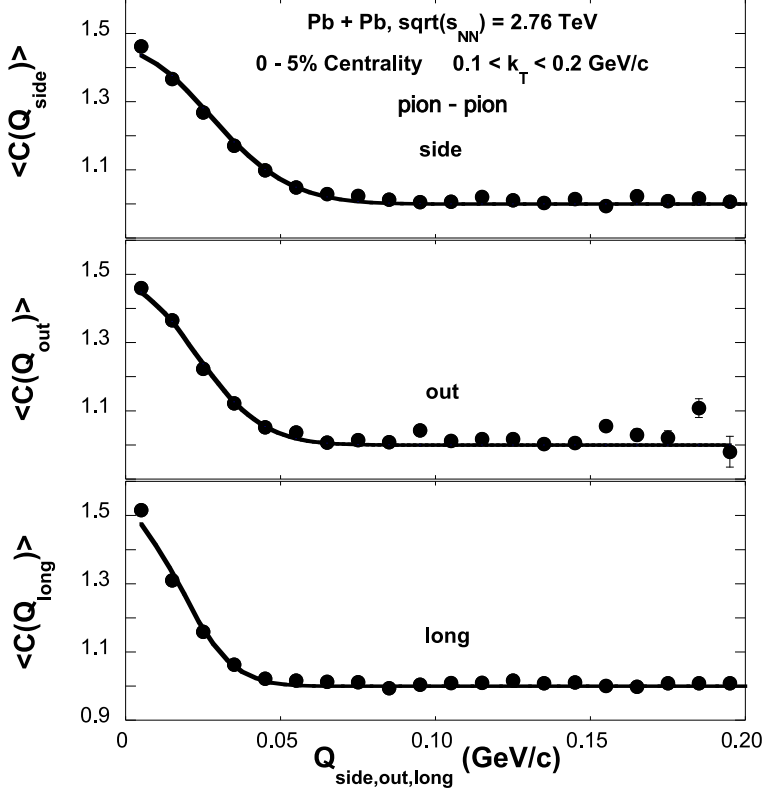


FIG. 5. Sample two-pion correlation function with Gaussian fit projected onto the Q_{out} , Q_{side} , and Q_{long} axes from the model. The collision centrality is 0 – 5% and the k_T bin is 0.1 – 0.2 GeV/c.

on k_T for centrality 0 – 5% and $-1 < \eta < 1$ for the full calculation compared with the calculation with rescattering turned off. For the full calculation, the radius parameters are all predicted to decrease with increasing k_T showing the effects of “flow” as has been observed in RHIC $Au + Au$ collisions and elsewhere [19, 20]. The overall scales of R_{side} and R_{out} predicted for $Pb + Pb$ are comparable to those seen in RHIC $Au + Au$ collisions, whereas R_{long} is predicted to be about 25% larger than at RHIC[20]. The λ -parameter is seen to be mostly independent of k_T with a value of about 0.6, which is significantly less than the “ideal HBT case” of $\lambda = 1$. The main effect causing $\lambda < 1$ in the model is the presence of long-lived resonances such as η and η' which decay into pions late in the collision thus suppressing the correlation function. Looking at the radius parameters with rescattering turned off in Figure 6, it is seen that their dependence on k_T mostly disappears and their scales are significantly reduced compared with the full calculation, showing the strong influence that rescattering has on the HBT parameters in this model. Comparing

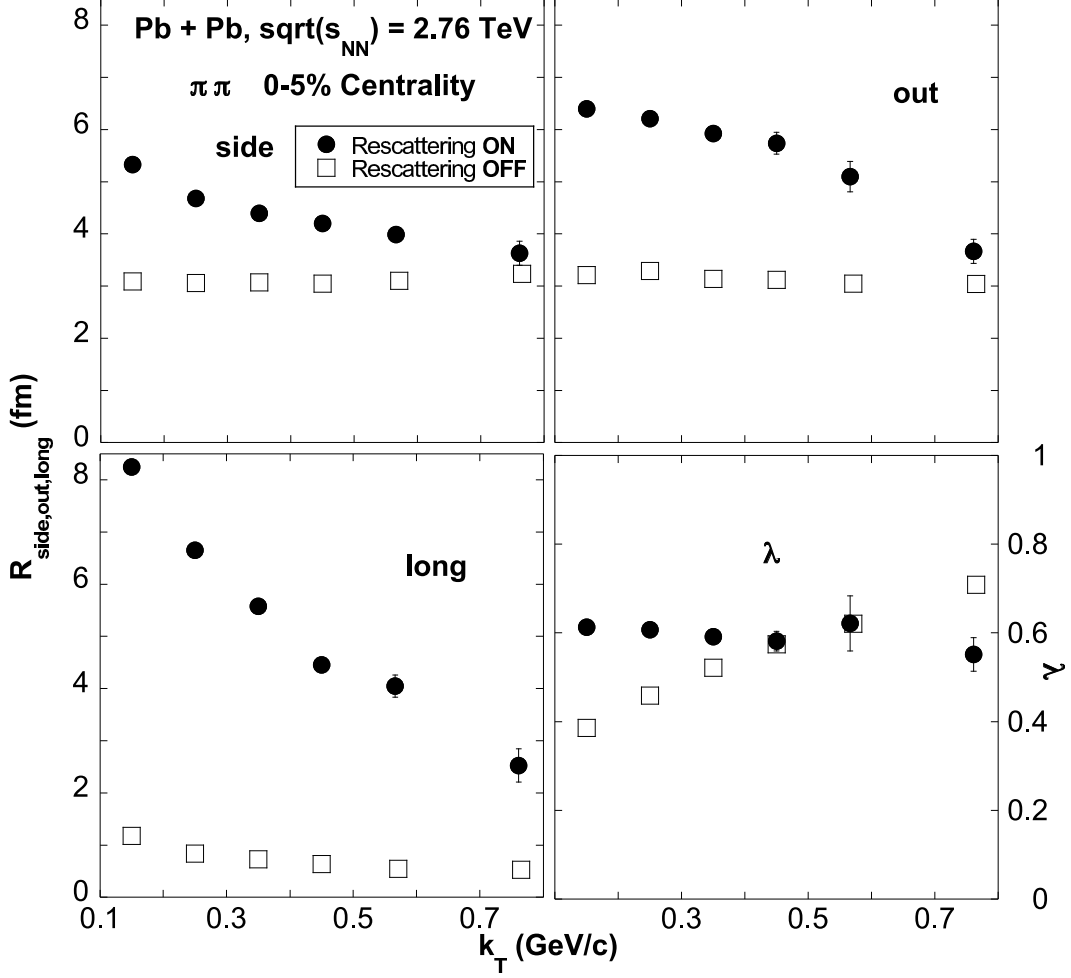


FIG. 6. Model pion source parameters vs. k_T for $Pb+Pb$ collisions, 0–5% centrality, $-1 < \eta < 1$, and with and without rescattering turned on.

λ -parameters, in the case with rescattering turned off the λ -parameter is seen to increase with increasing k_T unlike for the full calculation. An explanation for this behavior is that with rescattering turned off, the pion source is less Gaussian than with rescattering turned on and thus the λ -parameter tries to compensate in the fit for this effect.

Figure 7 compares the model pion source parameters vs. k_T for $Pb+Pb$ collisions, where $-1 < \eta < 1$, for the two centralities 0–5% and 62–72%. Tables I and II give the values for the plots in Figure 7. The more peripheral centrality case, i.e. 62–72%, is seen to have some qualitative similarities with the “Rescattering OFF” calculation shown in Figure 6, in that the radius parameters are seen to have weaker dependences on k_T than for the more central case, i.e. 0–5%, and are significantly smaller in magnitude. The λ -parameter k_T

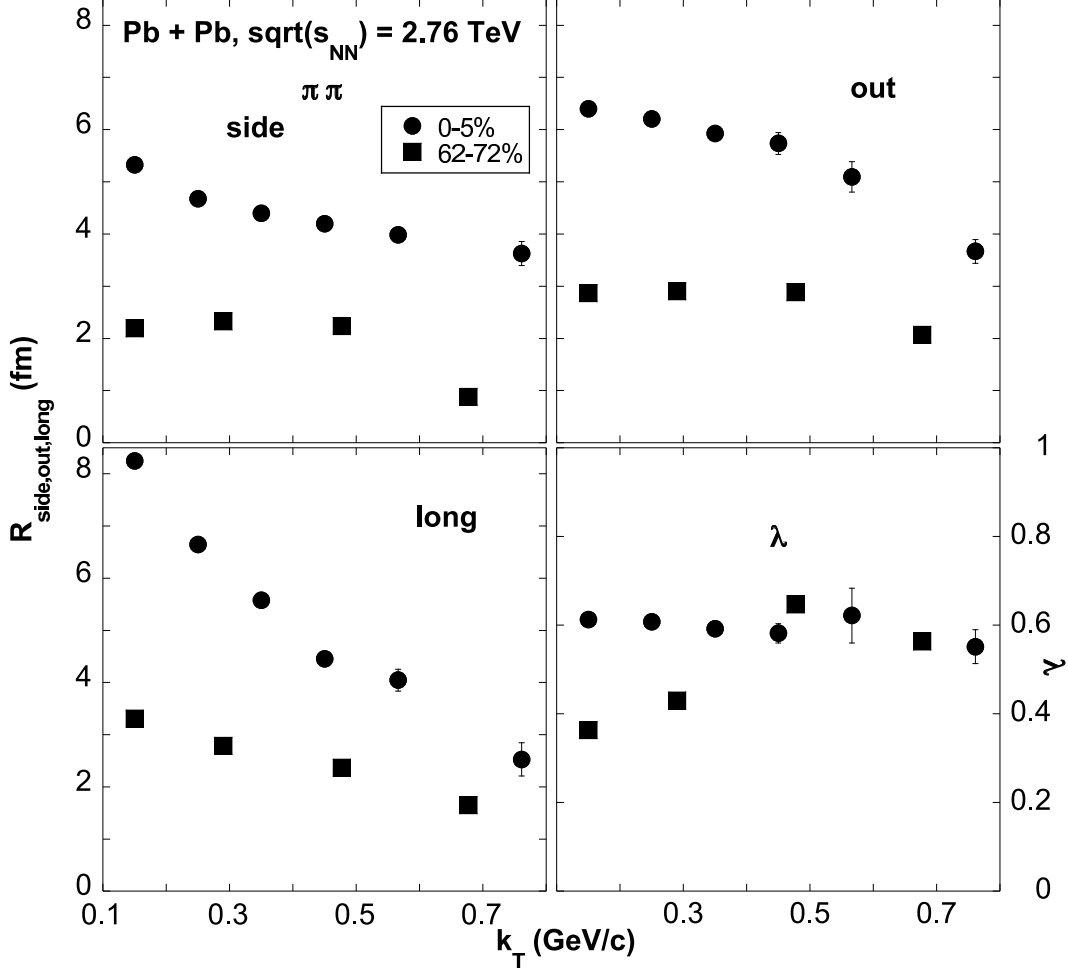


FIG. 7. Model pion source parameters vs. k_T for $Pb + Pb$ collisions, $-1 < \eta < 1$, 0 – 5% and 62 – 72% centralities.

dependence for the peripheral case also resembles that for the “Rescattering OFF” case in that λ more or less increases with increasing k_T as opposed to being mostly independent of k_T as for the full-calculation central case. The explanation for the similarities between the peripheral case and the “Rescattering OFF” case is due to the smaller particle multiplicity for the peripheral collisions and thus less rescattering present than for the central case, determined by the smaller initial geometric overlap of the projectile-target system in the peripheral case.

Model predictions have also been made for two-kaon HBT as shown in Figures 8 and 9. Figure 8 shows a sample two-kaon correlation function with Gaussian fit projected onto the Q_{out} , Q_{side} , and Q_{long} axes from the model for the collision centrality 0 – 5%, $-1 < \eta < 1$

TABLE I. Model pion source parameters vs. k_T for $\sqrt{s_{NN}} = 2.76$ TeV $Pb + Pb$ collisions, $-1 < \eta < 1$, 0 – 5% centrality.

| k_T range (GeV/c) | $\langle k_T \rangle$ (GeV/c) | λ | R_{side} (fm) | R_{out} (fm) | R_{long} (fm) |
|------------------------|----------------------------------|-------------------|--------------------|-------------------|--------------------|
| 0.10 – 0.20 | 0.15 | 0.613 ± 0.000 | 5.33 ± 0.00 | 6.40 ± 0.00 | 8.25 ± 0.00 |
| 0.20 – 0.30 | 0.25 | 0.608 ± 0.007 | 4.68 ± 0.05 | 6.21 ± 0.07 | 6.65 ± 0.06 |
| 0.30 – 0.40 | 0.35 | 0.592 ± 0.003 | 4.40 ± 0.07 | 5.93 ± 0.11 | 5.58 ± 0.05 |
| 0.40 – 0.50 | 0.45 | 0.582 ± 0.022 | 4.20 ± 0.06 | 5.74 ± 0.21 | 4.46 ± 0.06 |
| 0.50 – 0.70 | 0.57 | 0.622 ± 0.062 | 3.99 ± 0.13 | 5.10 ± 0.29 | 4.05 ± 0.21 |
| 0.70 – 1.00 | 0.76 | 0.552 ± 0.038 | 3.63 ± 0.23 | 3.67 ± 0.23 | 2.53 ± 0.32 |

TABLE II. Model pion source parameters vs. k_T for $\sqrt{s_{NN}} = 2.76$ TeV $Pb + Pb$ collisions, $-1 < \eta < 1$, 62 – 72% centrality.

| k_T range (GeV/c) | $\langle k_T \rangle$ (GeV/c) | λ | R_{side} (fm) | R_{out} (fm) | R_{long} (fm) |
|------------------------|----------------------------------|-------------------|--------------------|-------------------|--------------------|
| 0.10 – 0.20 | 0.15 | 0.364 ± 0.003 | 2.20 ± 0.02 | 2.87 ± 0.01 | 3.31 ± 0.02 |
| 0.20 – 0.40 | 0.29 | 0.430 ± 0.004 | 2.33 ± 0.01 | 2.91 ± 0.02 | 2.79 ± 0.02 |
| 0.40 – 0.60 | 0.48 | 0.647 ± 0.009 | 2.24 ± 0.06 | 2.89 ± 0.05 | 2.37 ± 0.07 |
| 0.60 – 1.00 | 0.68 | 0.564 ± 0.006 | 0.88 ± 0.03 | 2.07 ± 0.03 | 1.65 ± 0.03 |

and k_T bin 0.1 – 1.0 GeV/c. The Gaussian fit is seen to provide a reasonable fit to the model correlation function. Figure 9 presents a comparison of model pion and kaon source parameters vs. m_T for $Pb + Pb$ collisions, $-1 < \eta < 1$, centralities 0 – 5% and 62 – 72%. Table III gives the values for the two-kaon source parameters plotted in Figure 9. A large k_T bin of $0.10 < k_T < 1.00$ GeV/c with an average k_T of $\langle k_T \rangle = 0.39$ GeV/c was used for the two-kaon calculations in order to obtain reasonable statistical errors from the 3200 event minimum bias $Pb + Pb$ run used in the present study. Also, while a pseudorapidity range of $-1 < \eta < 1$ was used for the 0 – 5% centrality two-kaon calculation, a range of $-4 < \eta < 4$ was used for the 62 – 72% centrality two-kaon calculation in order to obtain reasonable statistical errors. As seen in Figure 9, the two-kaon calculations obey “ m_T -

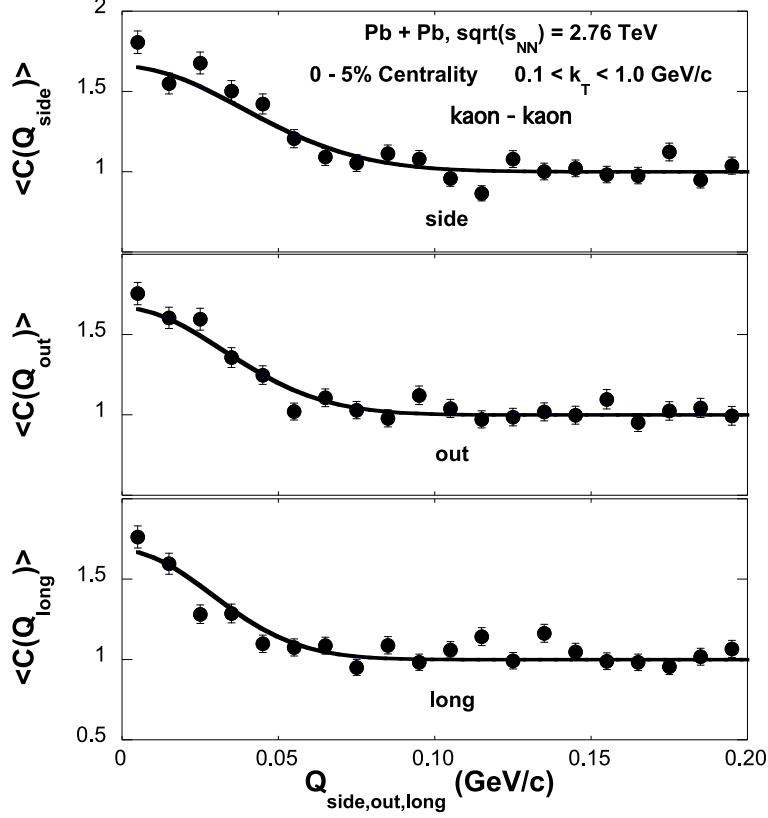


FIG. 8. Sample two-kaon correlation function with Gaussian fit projected onto the Q_{out} , Q_{side} , and Q_{long} axes from the model. The collision centrality is 0 – 5% and the k_T bin is 0.1 – 1.0 GeV/c.

TABLE III. Model kaon source parameters vs. centrality bin for $\sqrt{s_{NN}} = 2.76$ TeV $Pb + Pb$ collisions, $0.10 < k_T < 1.00$ GeV/c ($\langle k_T \rangle = 0.39$ GeV/c).

| Centrality bin | λ | R_{side} (fm) | R_{out} (fm) | R_{long} (fm) |
|----------------|-------------------|--------------------|-------------------|--------------------|
| 0 – 5% | 0.781 ± 0.030 | 3.60 ± 0.24 | 4.47 ± 0.16 | 4.51 ± 0.35 |
| 62 – 72% | 0.547 ± 0.054 | 2.04 ± 0.26 | 2.50 ± 0.13 | 2.49 ± 0.49 |

scaling” reasonably well with the two-pion calculations considering the large k_T bin that was necessary to use for the kaons.

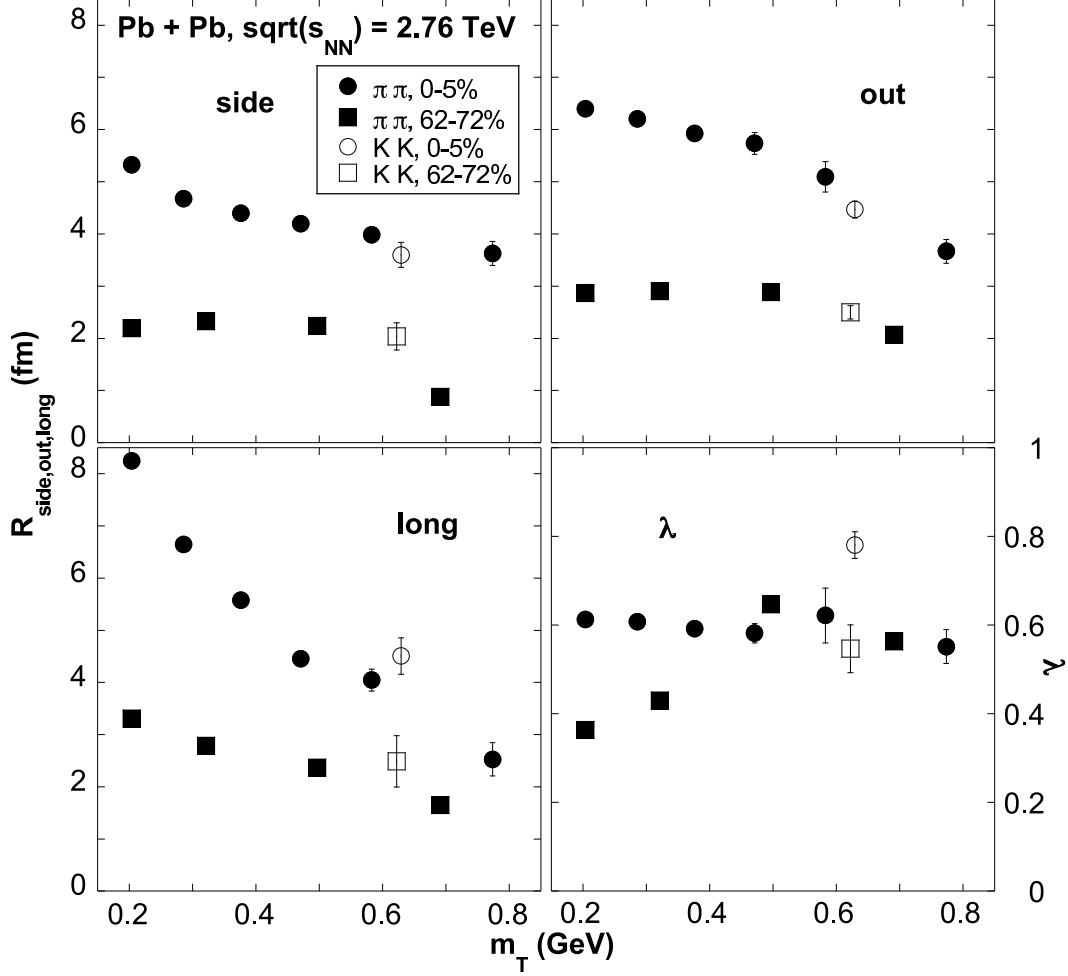


FIG. 9. Comparison of model pion and kaon source parameters vs. m_T for $Pb + Pb$ collisions, $-1 < \eta < 1$, 0 – 5% and 62 – 72% centralities.

IV. SUMMARY AND CONCLUSIONS

A kinematic model based on the superposition of PYTHIA-generated $p + p$ collisions, relativistic geometry and final-state hadronic rescattering has been used in the present work to predict several hadronic observables in $\sqrt{s_{NN}} = 2.76$ TeV $Pb + Pb$ collisions. A short proper time for hadronization of $\tau = 0.1$ fm/c has been assumed as in previous studies with this model which have shown qualitative agreement with experiments. Predictions for rapidity and transverse momentum distributions, elliptic flow, and two-boson femtoscopy have been presented which will likely be among the first observables to be extracted from analyses of the first $Pb + Pb$ data from the LHC.

The most noticeable features of the predictions from the present model study which have been presented are summarized below:

- $dn/d\eta$ near mid-rapidity for charged particles in LHC $Pb + Pb$ collisions is predicted to be about 1200 for a 0 – 5% centrality window. This puts its value at the lower end of the range of predictions which have been recently made of 1500 – 4000 in central collisions using various extrapolations of RHIC experimental rapidity densities.
- The 0 – 5% centrality charged particle p_T distribution for $p_T > 5$ GeV/ c is predicted to be about two orders of magnitude larger at the LHC compared with RHIC.
- High- p_T suppression of the R_{AA} is predicted to be present in LHC $Pb + Pb$ collisions as has been seen in RHIC collisions.
- Elliptic flow for charged hadrons is predicted to be comparable to that seen in RHIC collisions.
- Two-pion HBT radius parameters from LHC $Pb + Pb$ are predicted to be comparable in scale to those from RHIC $Au + Au$ collisions for R_{side} and R_{out} , and 25% larger for R_{long} and are predicted to show decreasing magnitude with increasing k_T , i.e. “flow” effects. Also, two-kaon HBT radius parameters are predicted to show “ m_T -scaling.”

As mentioned earlier, these are “limiting case scenario” predictions from a model that only considers hadronic degrees of freedom, i.e. which assumes that only “ordinary” physics processes are taking place in these collisions. Of course the “best case scenario” will be that these predictions disagree wildly with the actual measured hadronic observables which will soon be extracted by LHC experiments and exotic phenomena will indeed be observed.

ACKNOWLEDGMENTS

The author wishes to acknowledge financial support from the U.S. National Science Foundation under grant PHY-0970048, and to acknowledge computing support from the Ohio Supercomputing Center.

[1] K. Aamodt *et al.* [ALICE Collaboration], JINST **3**, S08002 (2008).

- [2] T. J. Humanic, Phys. Rev. C **79**, 044902 (2009) [arXiv:0810.0621 [nucl-th]].
- [3] T. Sjostrand, L. Lonnblad, S. Mrenna and P. Skands, arXiv:hep-ph/0603175 (March 2006).
- [4] T. Csorgo and J. Zimanyi, Nucl. Phys. A **512**, 588 (1990).
- [5] T. J. Humanic, Phys. Rev. C **76**, 025205 (2007).
- [6] T. J. Humanic, Int. J. Mod. Phys. E **15**, 197 (2006).
- [7] T. J. Humanic, Phys. Rev. C **57**, 866 (1998).
- [8] M. Prakash, M. Prakash, R. Venugopalan and G. Welke, Phys. Rept. **227**, 321 (1993).
- [9] W. M. Yao *et al.* [Particle Data Group], J. Phys. G **33**, 1 (2006).
- [10] T. J. Humanic, Phys. Rev. C **73**, 054902 (2006).
- [11] K. Aamodt *et al.* [ALICE Collaboration], Eur. Phys. J. C **68**, 89 (2010) [arXiv:1004.3034 [hep-ex]].
- [12] B. B. Back *et al.*, [PHOBOS collaboration], Phys. Rev. Lett. **91**, 052303 (2003).
- [13] K. Adcox *et al.* [PHENIX collaboration], Nucl. Phys. A **757**, 184 (2005).
- [14] S. S. Adler *et al.* [PHENIX Collaboration], Phys. Rev. C **69**, 034910 (2004).
- [15] J. Adams *et al.* [STAR Collaboration], Phys. Rev. C **72**, 014904 (2005).
- [16] B. I. Abelev *et al.* [STAR Collaboration], Phys. Rev. C **77**, 054901 (2008).
- [17] R. Hanbury Brown and R. Q. Twiss, Nature **177**, 27 (1956).
- [18] T. J. Humanic, Phys. Rev. C **34**, 191 (1986).
- [19] M. A. Lisa, S. Pratt, R. Soltz and U. Wiedemann, Ann. Rev. Nucl. Part. Sci. **55**, 357 (2005).
- [20] J. Adams *et al.* [STAR Collaboration], Phys. Rev. C **71**, 044906 (2005).